1154–1161 Vol. 78 No. 5 ACTA GEOLOGICA SINICA Oct. 2004
http://www.geojournals.cn/dzxbcn/ch/index.aspx

Water Self-Softening Processes at Waterfall Sites

CHEN Jing'an[1], David Dian ZHANG[2], WANG Shijie[1] and XIAO Tangfu[1]
1 *State Key Laboratory of Environmental Geochemistry, Institute of Geochemistry, Chinese Academy of Sciences, Guiyang, Guizhou 550002; E-mail: jinganchen@vip.163.com*
2 *Department of Geography and Geology, University of Hong Kong, Pokfulam Road, Hong Kong*

Abstract Many rivers in tropical and subtropical karst regions are supersaturated with respect to $CaCO_3$ and have high water hardness. After flowing through waterfall sites, river water is usually softened, accompanied by tufa formation, which is simply described as a result of water turbulence in fast-flowing water. In this paper, a series of laboratory experiments are designed to simulate the hydrological conditions at waterfall sites. The influences of air-water interface, water flow velocity, aeration and solid-water interface on water softening are compared and evaluated on a quantitative basis. The results show that the enhanced inorganic CO_2 outgassing due to sudden hydrological changes occurring at waterfall sites is the principal cause of water softening at waterfall sites. Both air-water interface area and water flow velocity increase as a result of the "aeration effect", "low pressure effect" and "jet-flow effect" at waterfall sites, which greatly accelerates CO_2 outgassing and therefore makes natural waters become highly supersaturated with respect to $CaCO_3$, consequently resulting in much $CaCO_3$ deposition and reduction of water hardness. Aeration, rapidly increasing air-water interface area and water flow velocity, proves to be effective in reducing water hardness. This study may provide a cheap, safe and effective way to soften water.

Key words: water softening, CO_2 outgassing, $CaCO_3$ precipitation, waterfall site

1 Introduction

The total hardness of natural waters, as an important indicator of water quality, is defined as the sum of calcium and magnesium concentrations. It is often expressed as the equivalent amount of calcium carbonate that could be formed from calcium and magnesium in the solution (Yang et al., 1999). High hardness is harmful at domestic and industrial scale because substantive calcite may form and be accumulated when being heated in pipes, boilers and cooking utensils (Saurina et al., 2002). Moreover, high hardness of drinking water may increase the risk of some diseases such as atopic dermatitis (Miyake et al., 2004).

Many rivers in tropical and subtropical karst regions have high water hardness. However, it has been found that water hardness is reduced when the river water flows through waterfall sites, accompanied by calcite precipitation and tufa formation. This is referred to as self-softening processes. Study on the water self-softening processes may be helpful for finding effective water softening measures.

Precipitation of calcite in natural waters can be simply described by the following reaction:

$$Ca^{2+}+2HCO_3^- \Leftrightarrow CaCO_3\downarrow + CO_2\uparrow +H_2O \quad (1)$$

Generally, precipitation of calcite requires the waters to be 5 to 10 times supersaturation with respect to calcite because of the lack of free energy to create new surface areas, unavailability of reactive calcite to act as nucleation sites, and inhibition of PO_4^{3-}, Mg^{2+} and organic ligands (Berner, 1975; Reddy 1977; Dandurand et al. 1982; Buhmann and Dreybrodt 1987; Lorah and Herman 1988; Lebron and Suarez 1996). This is why river water can maintain high hardness while no calcite precipitation appears in many karst rivers. In the Colorado River system of the southwest United States, calcite precipitation is not detectable although the water reaches 4–6 times supersaturation with respect to calcite (Suarez 1983).

It is well known that high supersaturation of water with respect to calcite usually results from the removal of CO_2 from the water. Several studies have attributed the CO_2 removal to turbulence, mixing of different waters and metabolic uptake of CO_2 by photosynthetic plants (Jacobson and Usdowski, 1975; Chafetz and Folk, 1984; Herman and Lorah, 1987; Viles and Goudie 1990). Studies of waterfall tufa have shown that a great amount of inorganic CO_2 outgassing occurred at waterfall sites (Chafetz and Folk, 1984; Lorah and Herman 1988; Ford, 1989; Zhang et al., 2001; Drysdale et al., 2002). Through detailed field measurements of temperature, pH, calcium concentration and alkalinity of water samples from two small streams in Southwest Germany, Merz-Preiβ and

Riding (1999) found that the principal cause of supersaturation in fast-flowing streams is inorganic carbon dioxide outgassing while photosynthetic uptake of carbon dioxide and temperature effects are negligible. This is testified by the field observation that organisms exist along the entire river channel while hardness reduction and tufa deposition occur mainly at waterfall sites. However, hardness reduction or calcite precipitation at waterfall sites has been simply described as a result of water turbulence. Knowledge about how environmental conditions change at waterfall sites and how these changes affect water hardness is rather scarce. We believe the principal cause of hardness reduction is the sudden hydrological change occurring at waterfall sites. In this paper, a series of experiments are designed to simulate the hydrological conditions at waterfall sites, and various factors affecting water softening are evaluated quantitatively.

2 Experiments and Methods

Understanding the hydrological changes occurring at waterfall sites is the key to design simulating experiments and thus to investigate the factors controlling water softening. Three major changes occur when river channel flow approaches to a waterfall. Firstly, sudden changes in flow conditions at waterfall sites can lead to air entrainment, which is termed "natural aeration". In rivers, aeration can appear in high-velocity flow, plunging free-jet flow, the wakes of topographic irregularities on channel beds, and in hydraulic-jump configurations, which suck and trap air inside the water body and create many air bubbles (Chanson and Qiao, 1994; Chanson and Cummings, 1996; Chanson and Toombes, 2003). These conditions are most obvious at waterfall sites, where "white-water phenomena" occur. Here we call the phenomena induced by air entrainment as the "aeration effect".

Secondly, water pressure at high velocity at waterfall sites is reduced according to the Bernoulli effect. At lower pressures, dissolved gases can be released from water as tiny air bubbles according to the Henry's law. This results in air detrainment at waterfall sites and is called "low pressure effect".

Finally, the fast-flowing and falling water at waterfall sites is broken into many water droplets, small streams and sprays due to the initial jet-flow turbulence and to the shear forces of the surrounding air. We call this phenomenon "jet-flow effect".

The "aeration effect" creates air bubbles at waterfall sites that can greatly increase the size of the air-water interface area. The "low pressure effect" at high flow velocity not only creates bubbles and thus enlarges the air-water interface area, but also reduces CO_2 content in the water resulting from detraining of the dissolved gases from the water flow. The "jet-flow effect" usually results in much larger air-water interface area because the jet flows consist of sprays, droplets and broken streams (Chanson and Cummings, 1996; Zhang et al., 2001). Thus it can be seen that the main hydrological changes, occurring at waterfall sites as a result of these effects, are the enlargement of air-water interface area and the increase of water flow velocity. We believe these two hydrological changes are the major cause of water softening or calcite precipitation. In order to testify our hypothesis, a series of laboratory experiments were designed to simulate changes in air-water interface area and flow conditions at waterfall sites, and to evaluate quantitatively their influences on water softening.

In order to acquire quantitative data on water softening rates, we need to continuously monitor Ca^{2+} concentration changes. In fact, it is impossible to determine Ca^{2+} concentrations continuously and accurately during the simulating processes because the simulating conditions would be changed if a part of solution were taken out for Ca^{2+} concentration determination. Fortunately, conductivity, which along carbonate-depositing systems fluctuates primarily as a result of carbonate deposition (Drysdale et al., 2002), is often a good tracer of Ca^{2+} concentration variations in natural karst waters (Groleau et al., 2000; Drysdale et al., 2002). In order to testify whether conductivity variability can represent Ca^{2+} concentration variations, Ca^{2+} concentrations and conductivities of laboratory solutions with different Ca^{2+} concentrations were measured respectively on an atomic absorption spectrometer (PE5100) and a portable multi-parameter instrument (pIONneer 65). The good correlation between them (Fig. 1) suggests that conductivity can be used as a surrogate measure of Ca^{2+} concentrations. Ca^{2+} concentrations can be calculated according to the initial Ca^{2+} concentrations and the conductivity in the sample solutions. The water softening rates can be deduced from the Ca^{2+} concentration variations.

$CaCO_3$ solution for simulating experiments was prepared

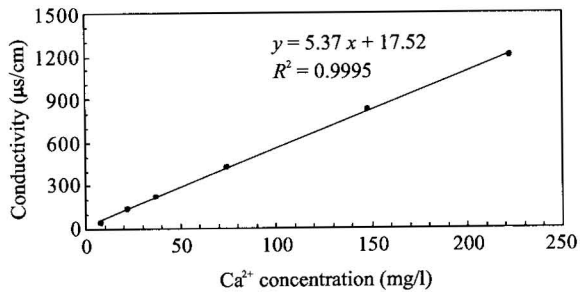

Fig. 1. Correlation between Ca^{2+} concentrations and conductivity in sample solutions.

by adding pure $CaCO_3$ grains in a 10-liter glass container full of distilled water. Pure CO_2 gas was then continuously pumped into the water for 72 hours. The $CaCO_3$ solution was passed through a 0.45-μm filter before used as sample solutions for experimental studies. The initial conductivities of the sample solutions range from 1050 to 1210 μs/cm.

All the following simulating experiments were carried out in a cultivator box set at 20°C in order to eliminate the influence of temperature on calcite precipitation. Changes of conductivity and pH in sample solutions were measured respectively on a portable multi-parameter instrument and an Orion 818 pH meter. The pH electrode was calibrated with pH 4.00 and 6.86 buffers every two hours.

1.1 Experiments on water softening processes

The first aim of this experiment is to systematically comprehend the water softening processes and the second aim is to examine the dependence of water softening on CO_2 outgassing. 550 ml of sample solution was put into a 11.21 cm-diameter cylindrical glass vessel with a water-surface area of 98.70 cm^2. The pH and conductivity of the sample solution were measured under stationary condition at time intervals of 10–20 minutes at the beginning in order to understand the fast-changing process, and at time intervals of 30–60 minutes when the sample solution showed only small fluctuations in pH and conductivity and finally appeared to reach equilibrium. The "equilibrated" solution was filtered through a 0.45-μm filter, and its Ca^{2+} concentrations were measured on an atomic absorption spectrometer

1.2 Air-water interface experiments

In order to evaluate quantitatively the influence of air-water interface on water softening and calcite precipitation, 550 ml of sample solution was put into three cylindrical glass vessels respectively with different water-surface areas of 55.65, 98.70 and 155.49 cm^2. These sample solutions had the same initial conductivity of 1052 μs/cm. Conductivity changes with time in the three sample solutions were measured on a portable multi-parameter instrument under stationary condition at time intervals of about 10 hours until the solutions appeared to stop precipitating. Ca^{2+} concentrations of the initial solutions and "equilibrated" solutions were measured on an atomic absorption spectrometer after they were filtered through a 0.45-μ m filter.

1.3 Flowing water experiments

The main aim of this experiment is to compare the water softening rates in standing and flowing waters. 550 ml of sample solution with an initial conductivity of 1031 μs/cm was put into a cylindrical glass vessel with a water-surface area of 55.65 cm^2. The glass vessel was put on a magnetic beater and a round magnetic rod with a length of 4 cm was put in the middle of the bottom of the vessel in order to make the solution move. When the magnetic beater worked, the sample solution had a rotation rate of 30 revolutions per second (i.e., an average flow velocity of 4 m/s). Conductivity variations were measured under flowing condition at time intervals of 10–20 minutes at the beginning and at time intervals of 30–60 minutes when the sample solution showed only small conductivity fluctuations. As a comparison, 550 ml of sample solution with an initial conductivity of 1049 μs/cm was put into a cylindrical glass vessel with the same water-surface area of 55.65 cm^2, and conductivity variations under stationary condition were monitored every 10–20 minutes at the beginning and every 30–60 minutes when the solution gradually approached to equilibrium.

1.4 Aeration experiments

The aim of this experiment is to evaluate quantitatively the influence of aeration on water softening. 550 ml of sample solution with an initial conductivity of 1047 μs/cm was put into a cylindrical glass vessel with a water-surface area of 55.65 cm^2. A bubble producer was designed to simulate the aeration effect. Airflow with normal atmospheric CO_2 partial pressure passed through a tube to the bubble producer in the sample solution to produce about 4000 air bubbles in 0.2 second, which was the period for each bubble to rise from the small holes of the producer to the water surface. Thus a total water-air interface area of about 602 cm^2 was added to the original air-water interface. Conductivity variations were measured under aeration condition at time intervals of 1–5 minutes at the beginning and at time intervals of 5–20 minutes when the sample solution gradually approached to equilibrium.

1.5 Solid-water interface experiments

In order to evaluate quantitatively the influence of solid-water interface on water softening and examine the relative importance of air-water interface and solid-water interface, 550 ml of sample solution was respectively put into two cylindrical glass vessels with the same surface area of 55.65 cm^2, one of which a calcite tablet with a surface area of 65.31 cm^2 was put in the middle of the bottom. The sample solutions had the same initial conductivity of 1180 μs/cm. Conductivity variations in these two solutions were monitored on a portable multi-parameter instrument under stationary condition at time intervals of about 10 hours until the solutions appeared to stop precipitating. Ca^{2+} concentrations of the initial solutions and "equilibrated" solutions were measured on an atomic absorption

spectrometer after they were filtered through a 0.45-μm filter in order to compare the water softening rates.

2 Results

2.1 Water softening processes observed under stationary condition

Variations in pH, conductivity and calcite precipitation rate with time under stationary condition are shown in Fig. 2, from which the following three stages were identified. The water softening rates can be reflected by the calcite precipitation rates because the reduction of water hardness resulted mainly from the precipitation of calcite.

2.1.1 The fast outgassing stage

This stage lasted about 25 hours and was characterized by the constant conductivity and a rapid increase in pH (Fig. 2). The P_{CO_2} difference between the ambient atmosphere and the sample solution resulted in quick diffusion of CO_2 from the water to the atmosphere, thus leading to the reduction of H^+ contents. This process can be shown by the reaction (2).

$$H^+ + HCO_3^- \Leftrightarrow H_2CO_3 \Leftrightarrow CO_2 \uparrow + H_2O \quad (2)$$

The supersaturation degree of water with respect to calcite is usually expressed by IAP/K_e, where IAP represents the ionic activity product and K_e represents the equilibrium constant of $CaCO_3$. One convenient method for the computation of IAP is:

$$IAP=(Ca^{2+})(CO_3^{2-})=$$
$$\{r_{Ca^{2+}}\times[Ca^{2+}]\times r_{HCO^{3-}}\times K_2\times Alk\}/(H^+) \quad (3)$$

where $r_{Ca^{2+}}$ and $r_{HCO^{3-}}$ are respectively the activity coefficients of Ca^{2+} and HCO_3^-, $[Ca^{2+}]$ is the Ca^{2+} concentrations, K_2 is the second dissociation constant for H_2CO_3, Alk is the alkalinity of the water, (H^+) is the H^+ activity defined through measuring pH values (pH =–log (H^+)). From equation (3), it can be easily seen that the supersaturation degree of water with respect to calcite increases with the reduction of H^+ contents. Detailed calculations showed the supersaturation degree of the sample solution with respect to calcite increases from 0.82 to 6.97 when pH rises from 6.22 at the beginning to 7.15 at the end of this stage. However, the constant conductivity of the sample solution indicated calcite precipitation did not commence. The calcite precipitation rate is almost equal to zero during this stage (Fig. 2).

2.1.2 The fast softening stage

This stage lasted about 170 hours and was characterized by a sharp drop in conductivity (Fig. 2), which reflected the rapid reduction of Ca^{2+} concentrations or water hardness. Because of the great loss of CO_2 during the fast outgassing stage, the supersaturation degree of water with respect to calcite rose to such a high level that the nucleation barrier can be overcome and the fast calcite precipitation started. Much H^+ was released into the solution during the processes of calcite precipitation, leading to the decrease of pH, which can be shown by equation (4). On the other hand, the released H^+ and HCO_3^- were gradually converted to CO_2 (Dreybrodt et al., 1997), leading to the reduction of H^+ contents, which can be shown by equation (5). When a balance was reached between the consumption of H^+ and its production, the pH value would remain stable. When the consumption rate of H^+ outpaced its production rate, the pH value would rise. When the conversion rate slowed down, the pH value would again decline. These processes alternately appeared during the whole stage and led to the frequent fluctuations of pH (Fig. 2). The calcite precipitation rates ranged from 8.0 to 92.0 μg/(l·min) during this stage with an average of 27.6 μg/(l·min) (Fig. 2).

$$Ca^{2+} + 2HCO_3^- \Leftrightarrow CaCO_3 \downarrow + HCO_3^- + H^+ \quad (4)$$

$$H^+ + HCO_3^- \Leftrightarrow CO_2 \uparrow + H_2O \quad (5)$$

2.1.3 The equilibrium stage

This stage was characterized by the relatively stable conductivity and pH value (Fig. 2). The rates of CO_2 outgassing and water softening slowed down because the P_{CO2} difference between the atmosphere and the sample solution decreased and the solution gradually approached to "equilibrium". The calcite precipitation rates were below 8.0 g/(l·min) with an average of 4.2 μg/(l·min) (Fig. 2).

Although the conductivity of the sample solution decreased continuously with time, the calcite precipitation rates fluctuated from time to time (Fig. 2). Two reasons may explain this phenomenon. Firstly, the sample solution was supersaturated with respect to calcite, so the conductivity showed a decreasing trend during the calcite

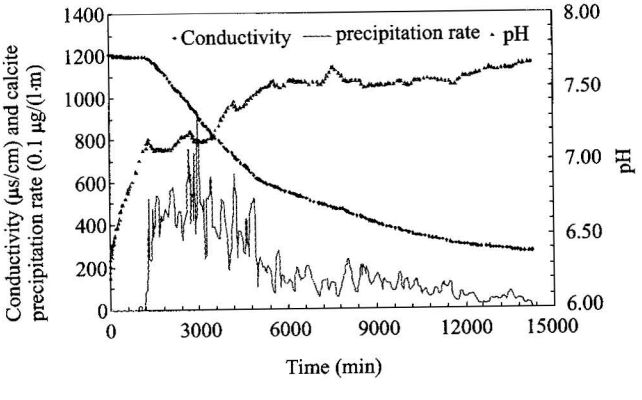

Fig. 2. Variations in conductivity, pH and calcite precipitation rate in sample solutions under stationary condition.

precipitation processes. Secondly, the supersaturation degree of water with respect to calcite varied as a result of frequent pH fluctuations (Fig. 2) according to equation (3), causing the calcite precipitation rates to vary from time to time.

2.2 The influence of the air-water interface on water softening

Variations in Ca^{2+} concentrations under stationary condition in the three sample solutions respectively with water-surface areas of 55.65, 98.70 and 155.49 cm^2 are shown in Fig. 3.

Obviously, an enlargement of air-water interface area not only shortened the period for the sample solution to reach equilibrium (Table 1), but also accelerated the water softening rates indicated by a faster decrease in Ca^{2+} concentrations (Fig. 3). The high correlation coefficient between the air-water interface area and the water softening rates (Fig. 4) suggests that the water softening rates, to a great extent, depend on the air-water interface area. Higher P_{CO2} in the water than in the ambient atmosphere drives CO_2 to diffuse quickly from the water to the air. All other things being equal, the larger the air-water interface area is, the faster the CO_2 will diffuse, the earlier the calcite precipitation will commence. In fact, this phenomenon can be well explained by the diffusion theory. The mass transfer rate of a chemical species across an interface is a function of the molecular diffusion coefficient, the negative gradient of gas concentration and the interface area. If the chemical of interest is volatile (e.g. CO_2), the gas transfer rate may be expressed as:

$$\frac{d}{dt}C_{gas} = K_L \times \alpha \times (C_{sat} - C_{gas}) \quad (6)$$

where C_{gas} is the dissolved gas concentrations, K_L is the mass transfer coefficient, α is the specific surface area and C_{sat} is the concentrations of the dissolved gas in water at equilibrium (Chanson, 1995; Chanson and Toombes, 2003). The mass transfer coefficient (K_L) is almost constant (Kawase and Moo-Yong, 1992). The specific surface area (α) is defined as the air-water surface area per unit volume of air and water (Chanson, 1995; Chanson and Toombes, 2003). In our experiments, the three sample solutions have the same volume, the same C_{sat} and the same initial C_{gas}, so the variations of the specific surface area can be represented by those of the air-water interface area, and equation (6) can be simplified as:

$$\frac{d}{dt}C_{gas} = K \times S \times (C_{sat} - C_{gas}) \quad (7)$$

where K is a constant and S is the air-water interface area. It is obvious from equation (7) that the air-water interface area decides the CO_2 outgassing rate, thus controlling the water softening rates.

Merz-Preiβ and Riding (1999) found that a greater

Table 1 Comparison of water softening rates in solutions with different air-water interface areas

Surface area (cm^2)	Initial Ca^{2+} concentration (mg/l)	Equilibrated Ca^{2+} concentration (mg/l)	Equilibrium time (h)	Water softening rate (mg/l·h)
55.65	254.6	38.8	312	0.69
98.70	254.6	38.4	247	0.88
155.49	254.6	37.9	173	1.25

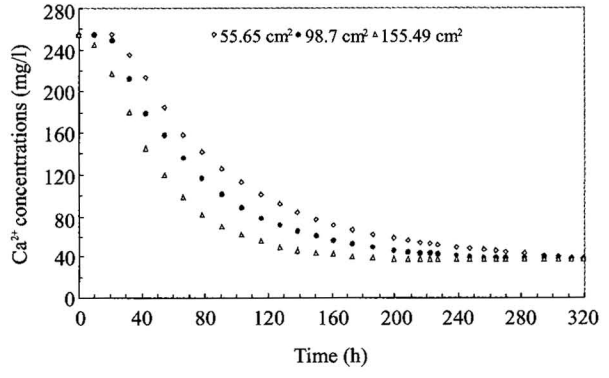

Fig. 3. Variations in Ca^{2+} concentrations in sample solutions with different air-water interface areas.

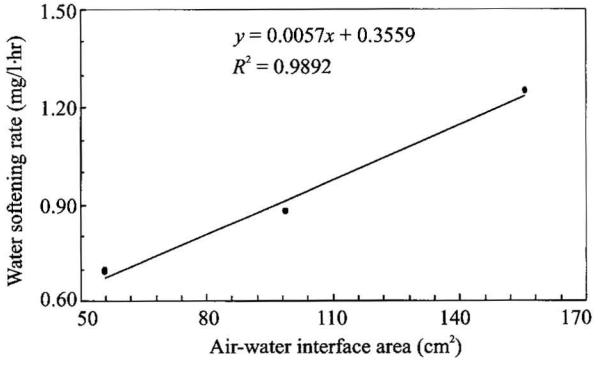

Fig. 4. Correlation between the air-water interface area and the water softening rates.

channel width (i.e., larger air-water interface area) allowed more rapid CO_2 outgassing while a narrower channel limited CO_2 outgassing and calcite precipitation. This provided direct field evidence for our experiment results.

2.3 The influence of flow velocity on water softening

Variations of Ca^{2+} concentrations in the sample solutions under stationary and flowing conditions are shown in Fig. 5.

From Fig. 5 and Table 2, it can be seen that the water softening rate in flowing water is more than four times larger than in stationary water, while the equilibrium time is only one-fourth of that in stationary water. This gives clear evidence for the influence of flowing conditions on water softening.

The behavior of a fluid under varying flowing conditions is described quantitatively by Bernoulli's law:

$$P + \frac{1}{2}\rho v^2 + \rho g h = [\text{constant}] \quad (8)$$

where P is the static pressure (N/m^2), ρ is the fluid density (kg/m^3), v is the velocity of fluid flow (m/s) and h is the height above a reference surface (m). Obviously, an increase in flow velocity will result in a decrease in static pressure from equation (8), so the water pressure is lower in a moving fluid than in a stationary fluid.

It is well known that the solubility of a gas in water decreases with decreasing pressure if the temperature stays constant according to the Henry's law, i.e.,

$$P = k \cdot C \quad (9)$$

where P is the static pressure (N/m^2), C is the gas concentration and k is the Henry's law constant, which is the same for the same temperature, gas and solvent. Therefore, dissolved gases can diffuse more quickly from flowing water than from stationary water. On the other hand, fast flowing water not only induces turbulence which can cause more effective collision among dissolved ions and, therefore, accelerates chemical reactions, but also reduces the thickness of diffusion boundary layers at both solid-water and air-water interfaces, which accelerates mass transfer through the two interfaces and thus speeds up calcite precipitation or water softening (Liu et al., 1995; Zhang et al., 2001). All these factors would jointly cause much earlier and faster hardness reduction in flowing water than in stationary water. This phenomenon also occurs in the field. Liu et al. carried out in-situ experiments to measure calcite deposition rates at the dam sites with fast water flow (0.5–2 m/s), as well as inside pools with still water in the Huanglong Ravine, China. The result showed that the depositional rates in fast flowing water were four times high those in still water although there was no difference in hydrochemistry (Liu et al., 1995). The good agreement between the field measurements and our laboratory observations provides convincing evidence that the flowing conditions can exert a large influence on water softening rates in natural waters.

2.4 The influence of aeration on water softening

Variations of Ca^{2+} concentrations with time in sample

Table 2 Comparison of water softening rates in solutions under stationary and flowing conditions

Flow condition	Initial Ca^{2+} concentration (mg/l)	Equilibrated Ca^{2+} concentration (mg/l)	Equilibrium time (hr)	Water softening rate (mg/l·h)
Stationary	254.6	38.8	312	0.69
Flowing	251.7	38.1	70	3.05

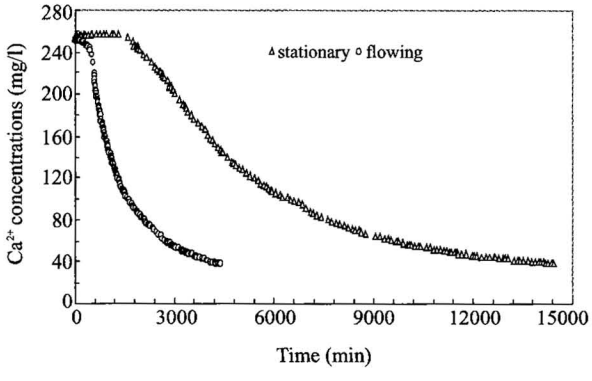

Fig. 5. Variations in Ca^{2+} concentrations in sample solutions under stationary and flowing conditions.

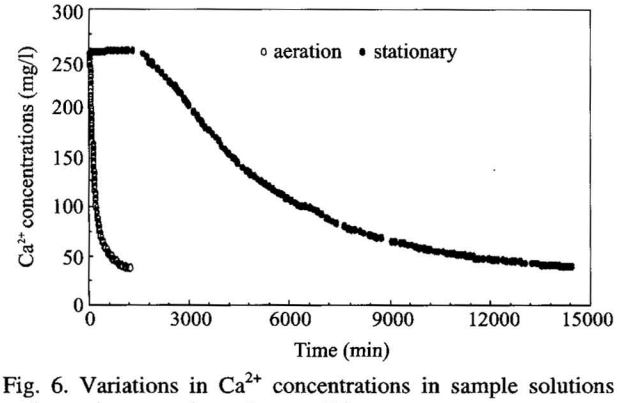

Fig. 6. Variations in Ca^{2+} concentrations in sample solutions under stationary and aeration conditions.

solutions under aeration and stationary conditions are shown in Fig. 6.

It is obvious from Fig. 6 that the Ca^{2+} concentrations of the sample solution decline very rapidly under aeration condition, dropping to 15% of the original level in 25 hours. In comparison, the Ca^{2+} concentrations of the sample solution under stationary condition show a much flatter decreasing trend. Detailed calculations show that the water softening rate under aeration condition is more than 12 times larger than in stationary water, while the equilibrium time is only one-twelfth of that in stationary water (Table 3).

On one hand, the bubbles from the holes increased the water-air interface area by about 602 cm^2. On the other hand, the rising bubbles induced strong water movement. These together greatly promoted CO_2 outgassing and accelerated water softening.

2.5 The influence of solid-water interface on water softening

Although the increase of solid-water interface area accelerated water softening (Fig. 7), it didn't affect the softening rate so much as the increase of air-water interface area (Fig. 3). Moreover, when river water flows over a waterfall, there will be a much greater increase in air-water interface area than in solid-water interface area. Therefore, the air-water interface is much more important in controlling water softening than the solid-water interface at waterfall sites. CO_2 outgassing plays a major role in reducing water hardness.

3 Discussion and Conclusions

Many rivers in tropical and subtropical karst regions are supersaturated with respect to $CaCO_3$ and have high water hardness because of the high contents of dissolved Ca^{2+} derived from groundwater. After river water flows through waterfall sites, $CaCO_3$ can be deposited and river water will be usually softened.

Our experiment results showed that the enlargement of air-water interface, the increase of water flow velocity and aeration condition can greatly accelerate CO_2 outgassing and lead to fast reduction of water hardness. At waterfall sites, both air-water interface area and water flow velocity tend to increase as a result of the "aeration effect", "low pressure effect" and "jet-flow effect", which will greatly accelerate CO_2 outgassing and, therefore, make natural waters become highly supersaturated with respect to $CaCO_3$, consequently resulting in much $CaCO_3$ deposition and fast reduction of water hardness. This is the major cause of water self-softening at waterfall sites and can be simply explained by the model shown in Fig. 8.

From the preceding discussions, we can see that CO_2 outgassing plays the most important role in water softening and an air-water interface is necessary in order to complete

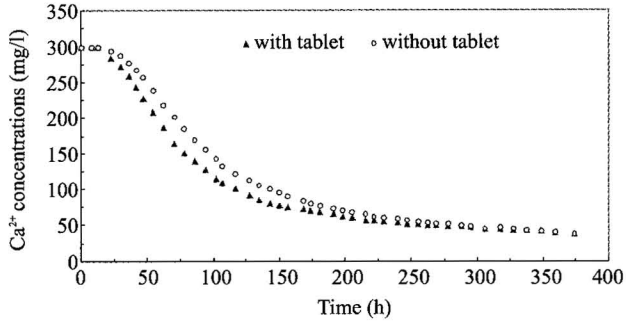

Fig. 7. Variations in Ca^{2+} concentrations in sample solutions with/without calcite tablet.

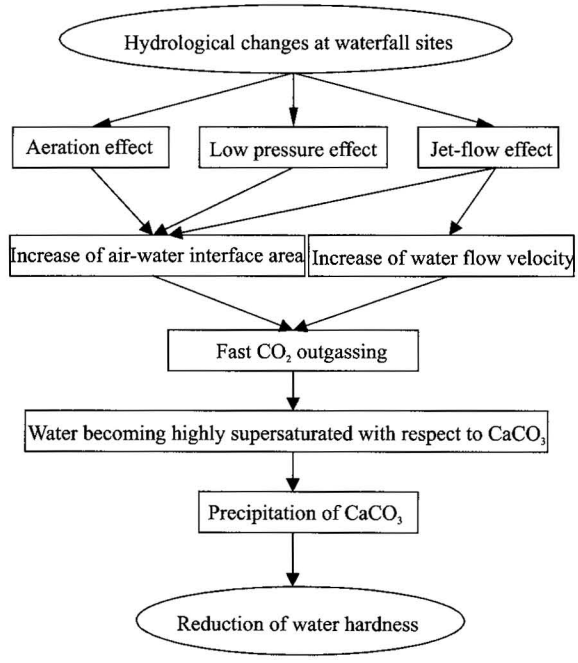

Figure 8 A simple model for water self-softening processes at waterfall sites.

Table 3 Comparison of water softening rates in solutions under stationary aeration conditions

Condition	Initial Ca^{2+} concentration (mg/l)	Equilibrated Ca^{2+} concentration (mg/l)	Equilibrium time (h)	Precipitation rate (mg/l·h)
Stationary	254.6	38.8	312	0.69
Aeration	254.6	37.1	25	8.70

the softening processes. However, there is no air-water interface in the tap water pipe, which is a closed system, so CO_2 outgassing does not occur and the water hardness remains unchanged from the pipe entrance to the exit. In order to reduce the hardness of tap water, necessary measures should be adopted before the water enters the pipe system. Aeration, which can greatly increase air-water interface and water flow velocity, has proved itself to be an effective way to reduce water hardness in our experiments. In fact, aeration processes have been successfully adopted in water treatment to remove harmful gases, but not yet been applied to softening water until now. What we have learned from this research may provide a cheap, safe and effective way for softening water.

Acknowledgements

This research was supported jointly by the CRCG Seed Grant of the University of Hong Kong and the National Natural Science Foundation of China (Nos. 90202003 and 40303014). We thank anonymous reviewers for their helpful comments and Professor Xu Zhongluen for correcting the English manuscript.

Manuscript received June 25, 2004
accepted July 26, 2004
Edited by Liu Xinzhu

Reference

Berner, R.A., 1975. The role of magnesium in the crystal growth of calcite and aragonite from seawater. *Geochim Cosmochim Acta*, 39: 489–504.

Buhmann, D., and Dreybrodt, W., 1987. Calcite dissolution kinetics in the system H_2O-CO_2-$CaCO_3$ with participation of foreign ions. *Chemi. Geol.*, 64: 89–102.

Chafetz, H.S., and Folk, R.L., 1984. Travertine: depositional morphology and the bacterially constructed constituents. *J. Sedimentary Petrology*, 54: 289–316.

Chanson, H., and Cummings, P.D., 1996. Air-water interface area in supercritical flows down small slope chutes. *Department of Civil Engineering Research Series No.CE151*, University of Queensland.

Chanson, H., and Qiao, G.L., 1994, Air bubble entrainment and gas transfer at hydraulic jump. *Department of Civil Engineering Research Series No.CE149*, University of Queensland.

Chanson, H., and Toombes, L., 2003. Strong interactions between free-surface aeration and turbulence in an open channel flow. *Experimental Thermal and Fluid Science*, 27: 525–535.

Chanson, H., 1995. Air-water gas transfer at hydraulic jump with partially developed inflow. *Water Research*, 29: 2247–2254.

Dandurand, J.L., Gout, R., Hoefs, J., Menschel, G. Schott, J., and Usdowski, E., 1982. Kinetically controlled variations of major components and carbon isotopes in a calcite-precipitating spring. *Chemi. Geol.*, 36: 299–315.

Dreybrodt, W., Elsenlohr, L., Madry, B., and Ringer, S., 1997. Precipitation kinetics of calcite in the system CaCO3-H_2O-CO_2: The conversion to CO_2 by the slow process $H^+ + HCO_3^- \rightarrow CO_2 + H_2O$ as a rate limiting step. *Geochimi. Cosmochim. Acta*, 361: 3897–3904.

Drysdale, R.N., Taylor, M.P., and Ihlenfeld, C., 2002. Factors controlling the chemical evolution of travertine-depositing rivers of the Barkly karst, northern Australia. *Hydrological Processes*, 16: 2941–2962.

Ford, T.D., 1989. Tufa: a freshwater limestone. *Geology Today*, 5: 60–63.

Groleau, A., Sarazin, G., Vincon-Leite, B., Tassin, B., and Quiblier-Lloberas, C., 2000. Tracing calcite precipitation with specific conductance in a hard water alpine lake. *Water Research*, 34: 4151–4160.

Herman, J.S., and Lorah, M.M., 1987. CO_2 outgassing and calcite precipitation in Falling Spring Creek, Virginia, USA. *Chemi. Geol.*, 62: 251–262.

Jacobson, R.L., and Usdowski, E., 1975. Geochemical controls on a calcite precipitating spring. *Contributions to Mineralogy and Petrology*, 51: 65–74.

Kawase, Y., and Moo-Yong, M., 1992. Correlations for liquid-phase mass transfer coefficients in bubble column reactors with Newtonian and non-Newtonian fluids. *Canadian J. Chemi. Eng.*, 70: 48–54.

Lebron, I., and Suarez, D.L., 1996. Calcite nucleation and precipitation kinetics as affected by dissolved organic matter at 25℃ and pH > 7.5. *Geochim. Cosmochim. Acta*, 60: 2765–2276.

Liu, Z., Svensson, U., Dreybrodt, W., Yuan, D.X., and Buhmann, D., 1995. Hydrodynamic control of inorganic calcite precipitation in Huanglong Ravine, China: field measurements and theoretical prediction of deposition rates. *Geochim. Cosmochim. Acta*, 59: 3087–3097.

Lorah, M.M., and Herman, J.S., 1988. The chemical evolution of a travertine-depositing stream: Geochemical processes and mass transfer reactions. *Water Resources Res.*, 24: 1541–1552.

Merz-Prei β , M., and Riding, R., 1999. Cyanobacterial tufa calcification in two freshwater streams: ambient environment, chemical thresholds and biological processes. *Sedimentary Geol.*, 126: 103–124.

Miyake, Y., Yokoyama, T., Yura, A., Iki, M., and Shimizu, T., 2004. Ecological association of water hardness with prevalence of childhood atopic dermatitis in a Japanese urban area. *Environmental Res.*, 94: 33–37.

Reddy, M.M., 1977. Crystallization of calcium carbonate in presence of trace concentration of phosphorus-contained anions, I, inhibition of phosphate and glycerophorus ions at pH 8.8 and 25°C. *J. Crystal Growth*, 41: 287–295.

Saurina, J., Aviles, E.L., Moal, A.L., and Cassou, S.H., 2002. Determination of calcium and total hardness in natural waters using a potentiometric sensor array. *Analytica Caca*, 464: 89–98.

Suarez, D.L., 1983. Calcite supersaturation and precipitation kinetics in the lower Colorado River, All-American Canal, and East Highland Canal. *Water Resource Res.*, 19: 653–661.

Viles, H.A., and Goudie, A.S., 1990. Tufas, Travertines and allied carbonate deposits. *Progress Phys. Geogr.*, 14: 19–41.

Yang, C.Y., Chiu, H.F., Cheng, M.F., Tsai, S.S., Hung, C.F., and Lin, M.C., 1999. Esophageal cancer mortality and total hardness levels in Taiwan's drinking water. *Environmental Res.*, 81: 302–308.

Zhang, D., Zhang, Y., Zhu, A., and Chen, X., 2001. Physical mechanisms of river waterfall tufa (travertine) formation. *J. Sedimentary Res.*, 71: 205–216.